Int J Adv Manuf Technol
DOI 10.1007/s00170-012-3898-5

ORIGINAL ARTICLE

Calibration of an articulated CMM using stochastic approximations

Ibrahim A. Sultan · Prajeesh Puthiyaveettil

Received: 25 July 2011 / Accepted: 3 January 2012

Abstract A coordinate measuring machine (CMM) is meant to digitise the spatial locations of points and feed the resulting measurements to a CAD system for storing and processing. For reliable utilisation of a CMM, a calibration procedure is often undertaken to eliminate the inaccuracies which result from manufacturing, assembly and installation errors. In this paper, an Immersion digitizer coordinate measuring machine has been calibrated using an accurately manufactured master cuboid fixture. This CMM has been designed as an articulated manipulator to enhance its dexterity and versatility. As such, the calibration problem is tackled with the aid of a kinematic model similar to those employed for the analysis of serial robots. In addition, a stochastic-based optimisation technique is used to identify the parameters of the kinematic model in order for the accurate performance to be achieved. The experimental results demonstrate the effectiveness of this method, whereby the measuring accuracy has been improved considerably.

Keywords CMM · Robots · Calibration · Accuracy · Digitization · CAD

1 Introduction

In the context of this paper, positioning accuracy of a kinematic structure is the difference between its actual and calculated positions. This difference is attributed to both geometric and non-geometric factors. The geometric factors are manifested by the deviation of the structure kinematic parameters from the values stored in the mathematical model. On the other hand, the non-geometric factors are represented by such notions as link flexibility and sensor offsets. Positioning accuracy can be improved by proper calibration techniques, which consider both geometric and non-geometric sources of error, as evident by the works of many authors, e.g. Judd and Knasinsky [7], Driels and Pathre [3], Khalil and Besnard [8] and Bai and Wang [1].

Some methods which have been proposed in the literature to calibrate manipulators are adequately simple and efficient to be considered for application in the field of coordinate measuring machine (CMM). For example, Veitschegger and Wu [18] designed and used a special tool, based on an accurately machined plate equipped with a set of precisely located holes, to calibrate a PUMA 560 robot. Similarly, Lim and Burdekin [10] used a precisely machined artefact for CMM calibration. This artefact was aligned precisely at 17 positions for an adequate number of data points to be collected. Also, Foulloy and Kelly [4] report a method which employs a specially machined cube equipped with 25 precision holes and an accurate insertion tool for robot calibration. The paper by Sultan and Wager [17] presents an approach which allowed the robotic structure to rotate about one joint axis at a time in order for this specific axis to be individually located in space. The sequential application of this technique produced the required kinematic information for the whole structure. While suitable for robots, whose individual joints can be locked at any desired position, this method may not be applicable for CMM applications if such functionality is not provided.

In the current paper, a simplified approach is presented and applied for the calibration of the Immersion digitizer manipulator-like CMM [5]. This machine is accurate enough to be utilised in medical applications as evident by the work of Reisner et al. [12]. However, over a period of time, its accuracy may be adversely affected by relocation, overuse and environmental and working conditions. The basic premise in this paper is to calibrate the device by combining an inexpensive but accurately machined fixture with a kinematic model constructed as described by the well-known Denavit–

I. A. Sultan (✉) · P. Puthiyaveettil
School of Science, Information Technology and Engineering,
University of Ballarat,
PO Box 663, Ballarat, VIC 3353, Australia
e-mail: i.sultan@ballarat.edu.au

Published online: 17 January 2012

Hartenberg formulation [2]. Despite its obvious simplicity, this formulation has been shown, by authors such as Sultan and Wager [16] and Mooring et al. [11], to be mathematically unstable if used for calibration models which feature gradient-based optimisation techniques. In fact, the model's Jacobian matrix will become singular if two consecutive joint axes, on the kinematic structure, are parallel. On the other hand, the stochastic optimisation technique adopted in this paper does not require the use of a Jacobian matrix and as such is not expected to exhibit singular behaviour. This optimisation technique is referred to as simultaneous perturbation stochastic approximation (SPSA). This approach is efficient and suited for intricate optimisation application as abundantly explained in literature, e.g. the excellent papers by Spall [14] and the interesting application presented by Kothandaraman and Rotea [9].

2 Kinematic description of the IDCMM

The photo in Fig. 1 shows the manufactured structure of the Immersion digitizer coordinate measuring machine (IDCMM) featured in this paper. The machine, which has been patented by Schena and Rosenberg [13], is essentially a five-axis revolute-joint (i.e. 5R) serial manipulator with a high degree of dexterity. A displacement transducer is fitted to each joint axis to report the current value of joint angle to a software package provided by the manufacturer. The intended structure of the IDCMM consists of joints whose axes are either parallel or perpendicular in order to simplify the kinematic model of the machine. However, manufacturing and assembly errors may result in deviations from the intended kinematic structure. As such, Fig. 2 is provided to demonstrate a generic kinematical representation of a 5R serial manipulator similar to the CMM under study.

In Fig. 2, the centreline of each revolute joint is defined by a spatial axis, Z_i (i=1,2,…5). The centreline of the stylus is meant to coincide with the axis Z_6. However, the stylus tip, point P, is assumed not to fall on Z_6 in order for generality to be ensured. The relative positions of the joint axes with respect to each others may be formulated by using the well-known DH matrices which have been described by Denavit and Hartenberg [2]. A DH matrix is usually established to perform homogeneous transformation between two adjacent Cartesian frames as shown in Fig. 3.

In kinematical analysis, the Z-axes of frames are usually made to coincide with the joint axes, and the X_i-axis is the common normal directed from Z_i to Z_{i+1}. Generally, a frame, X_{i+1} Y_{i+1} Z_{i+1}, can be transformed into an adjacent frame, $X_iY_iZ_i$, by the following DH parameters:

θ_i which is the angle from X_i to X_{i+1}, as measured in a right-hand sense about Z_i

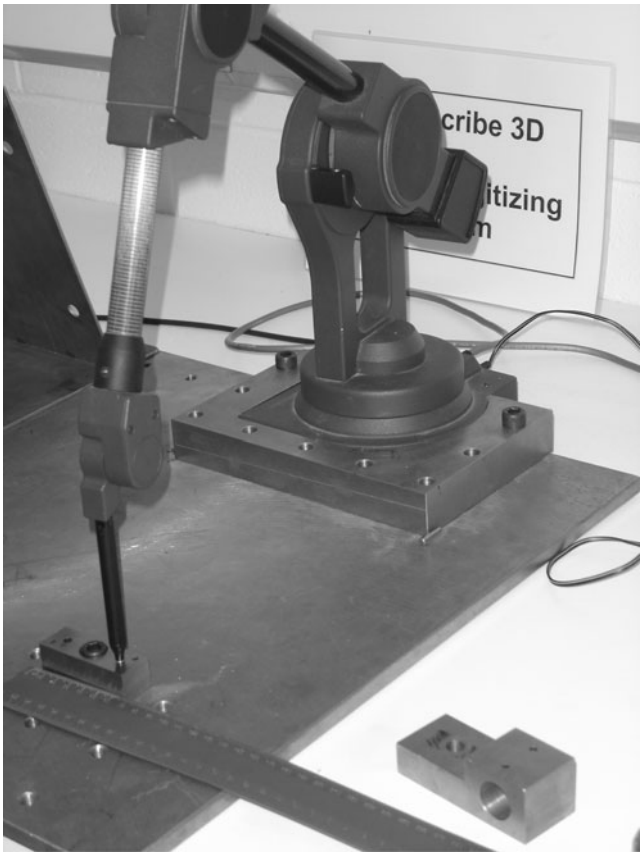

Fig. 1 Photograph of the CMM under study

α_i which is the angle from Z_i to Z_{i+1} as measured in a right-hand sense about X_{i+1}

d_i which is distance from X_i to X_{i+1}, as measured along Z_i

a_i which is the distance from Z_i to Z_{i+1}, as measured along X_{i+1}

For each revolute joint, all the DH parameters are constant, except θ_i, which varies with the rotational motion occurring about the joint axis. The DH matrix, $\mathbf{T}^i_{i+1}$, which performs the transformation from the frame number i+1 to the frame number i, is given as follows:

$$\mathbf{T}^i_{i+1} = \begin{bmatrix} \cos(\theta_i) & -\cos(\alpha_i)\sin(\theta_i) & \sin(\alpha_i)\sin(\theta_i) & a_i\cos(\theta_i) \\ \sin(\theta_i) & \cos(\alpha_i)\cos(\theta_i) & -\sin(\alpha_i)\cos(\theta_i) & a_i\sin(\theta_i) \\ 0 & \sin(\alpha_i) & \cos(\alpha_i) & d_i \\ 0 & 0 & 0 & 1 \end{bmatrix} \quad (1)$$

To this end, the overall matrix, $\mathbf{T}$, which expresses the stylus frame, $X_6Y_6Z_6$, with respect to the base frame, $X_1Y_1Z_1$, can be calculated as follows:

$$\mathbf{T} = \prod_{i=1}^{5} \mathbf{T}^i_{i+1} \quad (2)$$

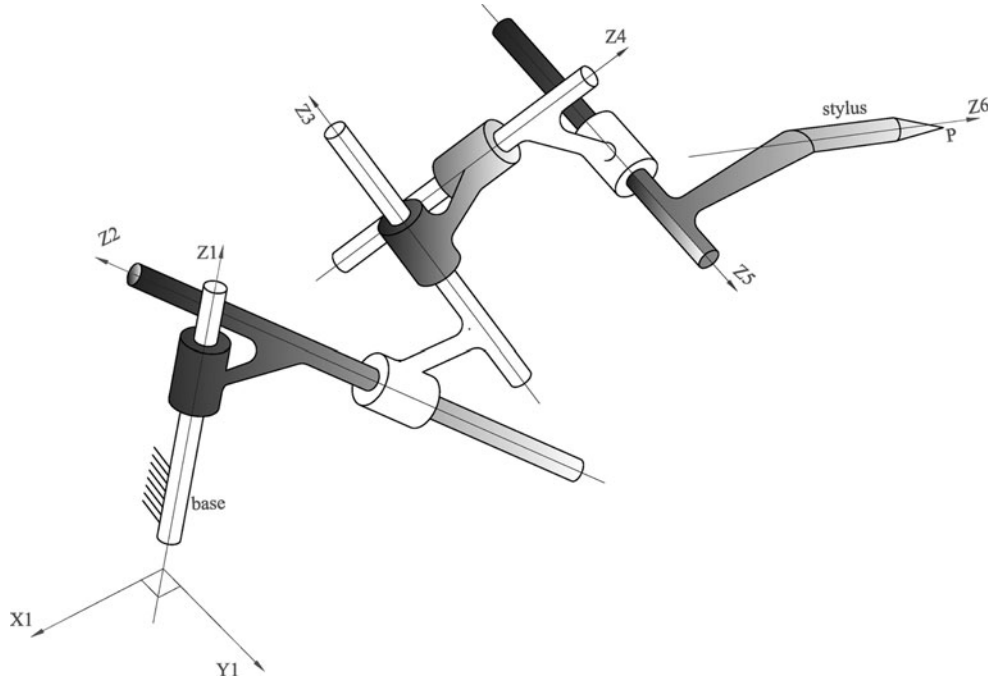

Fig. 2 A kinematical representation of the CMM under study

Let a unit vector, $\widehat{\mathbf{z}}_6$, be aligned with the stylus axis, Z_6. This unit vector may be expressed, with respect to the base frame, as the top three entries of the third column of the matrix **T** as follows:

$$\widehat{\mathbf{z}}_6 = [\,\mathbf{T}_{02} \quad \mathbf{T}_{12} \quad \mathbf{T}_{22}\,]^T \tag{3}$$

Moreover, the spatial position of the stylus tip can be expressed with respect to the base frame by a vector, $\mathbf{p}=[\mathbf{p}_x, \mathbf{p}_y, \mathbf{p}_z]$, which can be calculated as follows:

$$\begin{bmatrix} \mathbf{p}_x \\ \mathbf{p}_y \\ \mathbf{p}_z \\ 1 \end{bmatrix} = \mathbf{T} \begin{bmatrix} h_x \\ h_y \\ h_z \\ 1 \end{bmatrix} \tag{4}$$

where h_x, h_y and h_z are the x-, y- and z-coordinates of the stylus tip with respect to the frame $X_6Y_6Z_6$.

3 The SPSA approach

SPSA stands for simultaneous perturbation stochastic approximation as pointed out by Spall [14]. The approach is meant to minimise a loss function, $f(\mathbf{\Phi})$, which corresponds to a given design vector, $\mathbf{\Phi}$. This loss function can be expressed as follows:

$$f(\mathbf{\Phi}) = L(\mathbf{\Phi}) + \varepsilon(\mathbf{\Phi}) \tag{5}$$

where $L(\mathbf{\Phi})$ is the actual value of the function and $\varepsilon(\mathbf{\Phi})$ is the measurement noise.

Let an iterative procedure be undertaken to find the values of the design variables which will minimise the loss function. Assume that, at the start of iteration number k, the vector of design variables has been previously estimated as $\widehat{\mathbf{\Phi}}^k$ (where, in this context, the symbol $\widehat{\ }$ signifies estimates). To this end, the gradient, $g_q\left(\widehat{\mathbf{\Phi}}^k\right)$, of the loss function with respect to a specific design variable, $\mathbf{\Phi}_q$, may be approximated by the following expression:

$$g_q\left(\widehat{\mathbf{\Phi}}^k\right) = \frac{f\left(\widehat{\mathbf{\Phi}}^k + C_k\Delta^k\right) - f\left(\widehat{\mathbf{\Phi}}^k - C_k\Delta^k\right)}{2C_k\Delta_q^k} \tag{6}$$

where the entries of the vector Δ are randomly assigned the values of either +1 or −1 as generated, at every iteration, by a binary Bernoulli distribution. Mathematically, this is expressed as follows:

$$\Delta_q^k = \begin{cases} +1 & \text{with prob } 0.5 \\ -1 & \text{with prob } 0.5 \end{cases} \tag{7}$$

As such, the value of $\mathbf{\Phi}_q$ can be estimated, at the end of iteration k, by the following expression:

$$\widehat{\mathbf{\Phi}}_q^{k+1} = \widehat{\mathbf{\Phi}}_q^k - r_k g_q\left(\widehat{\mathbf{\Phi}}^k\right) \tag{8}$$

where $\widehat{\mathbf{\Phi}}_q^k$ is the estimated value of $\mathbf{\Phi}_q$ at the start of iteration number k. The scalar parameters, r_k and C_k, in Eqs. 6 and 8 are the sequence gains which are calculated at iteration number k as follows:

$$r_k = \frac{R}{(B+k)^{0.602}} \tag{9}$$

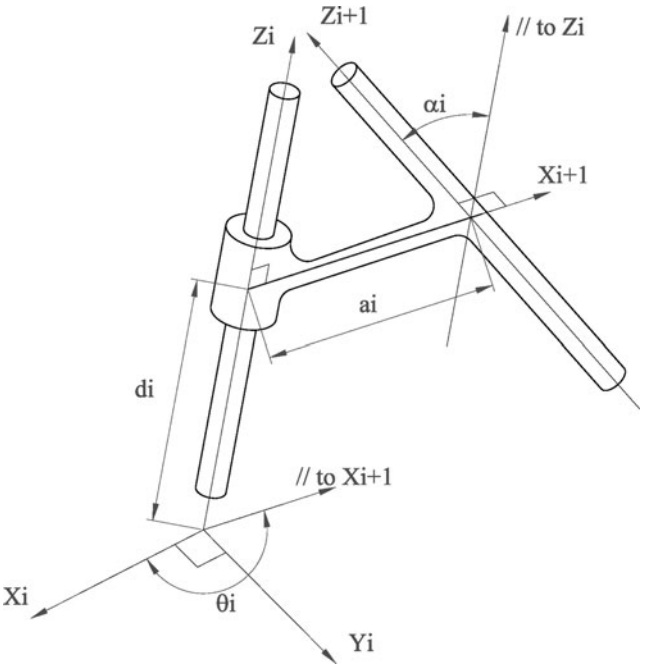

Fig. 3 The DH parameters

and

$$C_k = \frac{C}{k^{0.101}} \tag{10}$$

Spall [15] suggests that the stability constant, B in Eq. 9, may be calculated as $0.1K$, where K is the maximum allowed number of iterations which is set at the start of the procedure. Spall also presented in the same paper guidelines to inform the process of selecting numerical values for the constants, R and C, in Eqs. 9 and 10. The parameter C determines the process scale and, if set equal to the standard deviation of measurement noise, produces a smooth progression toward the optimal outcome. On the other hand, R may be set such that for the specific design variable, $\mathbf{\Phi}_s$, whose differential variation is expected to be the smallest, $r_0 g_s\left(\widehat{\mathbf{\Phi}}^0\right) \leq b$, where b is a small number specified by the user based on their familiarity with the problem at hand. In fact, high precision is not required for the values of R and C, and the process may boil down to a number of trial runs until reasonable values have been found to ensure smooth regression and an optimised outcome.

4 The calibration problem and procedure

When the IDCMM is employed to measure the position of the stylus tip in space, the measured values of the joint-axis sensor readings (i.e. θ_i, i=1,2,…,5) are reported to a computer package [6] designed to calculate the vector **p** which corresponds to the given joint angles as suggested by Eq. 4. Besides the joint angles, the elements of these vector depend on the 18 constant kinematic parameters of the structure, namely h_x, h_y, h_z, a_i, α_i and d_i (where i=1,2,…,5). The discrepancy which results from the actual physical values of these parameters, being slightly different from their intended values, is demonstrated by the measurement errors. A calibration procedure is, therefore, undertaken to find the actual values of these parameters and use them to calculate the vector **p**.

In addition to the aforementioned kinematic parameters, the work presented here considers possible error in the reading of each joint angle. For simplicity, this error is assumed to take the following linear form:

$$\gamma_i = f_i\theta_i + e_i \tag{11}$$

where γ_i replaces θ_i in the mathematical model and i=1,2,…,5. This implies that γ_i is regarded as the actual joint angle and θ_i is taken at the value reported by the joint sensor for this angle. In Eq. 11, e_i and f_i are unknown parameters which have to be found by the calibration procedure. The inclusion of e_i and f_i into the mathematical model increases the number of parameters, which are required to be found, from 18 to 28.

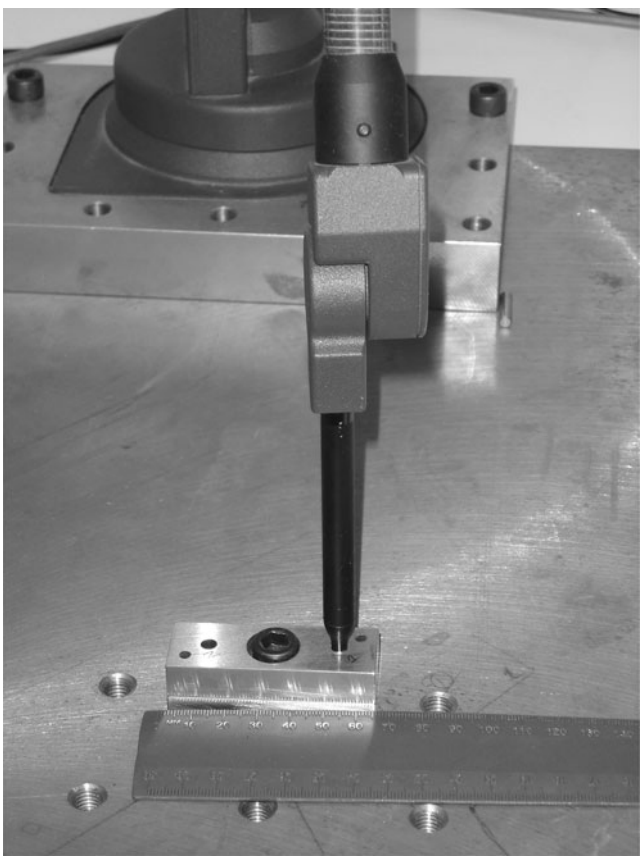

Fig. 4 The calibration cuboid with the stylus inserted

Table 1 Initial values of the model parameters

a_1=24.13 mm	α_1=89.8956°	d_1=210.82 mm	e_1=0	f_1=1
a_2=260.579 mm	α_2=358.8682°	d_2=−22.301 mm	e_2=0	f_2=1
a_3=13.716 mm	α_3=90.0824°	d_3=0.0762 mm	e_3=0	f_3=1
a_4=−10.16 mm	α_4=269.8956°	d_4=235.102 mm	e_4=0	f_4=1
a_5=−10.16 mm	α_5=270.088°	d_5=8.1026 mm	e_5=0	f_5=1
h_x=0 mm	h_y=0 mm	h_z=133.985 mm	D=40.05 mm	

The calibration procedure proposed in this paper employs a fixture which consists of a high precision cuboid with two wire-cut through holes of diameter 5.08 mm, located 40.05 mm apart. Figure 4 shows the measuring cuboid, as located next to a ruler, with the stylus inserted in one of its two holes.

The procedure involves moving the cuboid to a number of random locations in the measurement space whereby at each location, j, the stylus is inserted into the two holes in order for a zero-valued error function, $E_j(\boldsymbol{\Theta})$, to be calculated as follows:

$$E_j(\boldsymbol{\Theta}) = w_1\left(D - \left|\mathbf{p}_j^0 - \mathbf{p}_j^1\right|\right)^2 + w_2\left(1 - \hat{\mathbf{z}}_{6j}^0 \circ \hat{\mathbf{z}}_{6j}^1\right)^2 + w_3\left(\left(\hat{\mathbf{z}}_{6j}^0 \times \hat{\mathbf{z}}_{6j}^1\right)_x\right)^2 + w_4\left(\left(\hat{\mathbf{z}}_{6j}^0 \times \hat{\mathbf{z}}_{6j}^1\right)_y\right)^2 + w_5\left(\left(\hat{\mathbf{z}}_{6j}^0 \times \hat{\mathbf{z}}_{6j}^1\right)_z\right)^2 \quad (12)$$

where || is the Euclidian norm and the superscripts, 0 and 1, refer to the two holes, on the measuring cuboid, which are separated by the distance D. In Eq. 12, $w_i(l=1,2,\ldots,5)$ refer to weighting values assigned to the various terms of the error function. To account for possible manufacturing errors, the distance D was included in the analysis as an unknown parameter, which resulted in calibrating the measuring artefact itself. As such, the vector of unknown parameters, $\boldsymbol{\Theta}$ in Eq. 12, now holds 29 (rather than 28) entries.

In the error function shown by Eq. 12, the term $\left(D - \left|\mathbf{p}_j^0 - \mathbf{p}_j^1\right|\right)^2$ signifies the fact that the measured positions of the two cuboid holes, at any location number j, should be separated by a constant distance, D. Any deviation from that is a system error which the term endeavours to quantify. The remaining terms in Eq. 12 assert that the two axes $\hat{\mathbf{z}}_{6j}^0$ and $\hat{\mathbf{z}}_{6j}^1$ should be parallel at any location number j and endeavour to quantify deviations from parallelism (i.e. the dot product should be equal to 1 and the cross product should yield a zero vector).

Mathematically, the optimisation procedure involves the minimisation of a cost function, $F(\boldsymbol{\Theta})$, given as follows:

$$F(\boldsymbol{\Theta}) = \sum_1^M E_j(\boldsymbol{\Theta}) \quad (13)$$

where M is the total number of measuring events. As such, the problem is posed as follows:

$$\text{Minimize : } F(\boldsymbol{\Theta}) \qquad \text{Subjectto : } \boldsymbol{\Omega}_{\min} \le \boldsymbol{\Omega} \le \boldsymbol{\Omega}_{\max} \quad (14)$$

where $\boldsymbol{\Omega}$ is a sub-vector of $\boldsymbol{\Theta}$. The entries of $\boldsymbol{\Omega}$ are those design variables whose values have to be constrained as prescribed by the corresponding vectors $\boldsymbol{\Omega}_{\min}$ and $\boldsymbol{\Omega}_{\max}$.

Applying the approach of SPSA to the calibration problem at hand, the updated values of the design variable, $\boldsymbol{\Theta}_q^{k+1}$, which occupies position number q (where q=0,1,…,28) in the design vector is calculated at the end of iteration step number k by:

$$\boldsymbol{\Theta}_q^{k+1} = \boldsymbol{\Theta}_q^k - r_k \frac{F\left(\boldsymbol{\Theta}^k + C_k\Delta^k\right) - F\left(\boldsymbol{\Theta}^k - C_k\Delta^k\right)}{2C_k\Delta_q^k} \quad (15)$$

Table 2 Calculated values of the model parameters

a_1=24.357 mm	α_1=90.05°	d_1=211.240 mm	e_1=−0.123°	f_1=0.999
a_2=260.242 mm	α_2=359.885°	d_2=−22.256 mm	e_2=0.214°	f_2=1.009
a_3=13.600 mm	α_3=90.299°	d_3=−0.0762 mm	e_3=0.107°	f_3=1.001
a_4=−10.309 mm	α_4=270.172°	d_4=234.86 mm	e_4=0.917°	f_4=1.001
a_5=10.139 mm	α_5=270.459°	d_5=8.094 mm	e_5=0.080°	f_5=0.993
h_x=0.0008 mm	h_y=0.0012 mm	h_z=133.985 mm	D=40.05 mm	

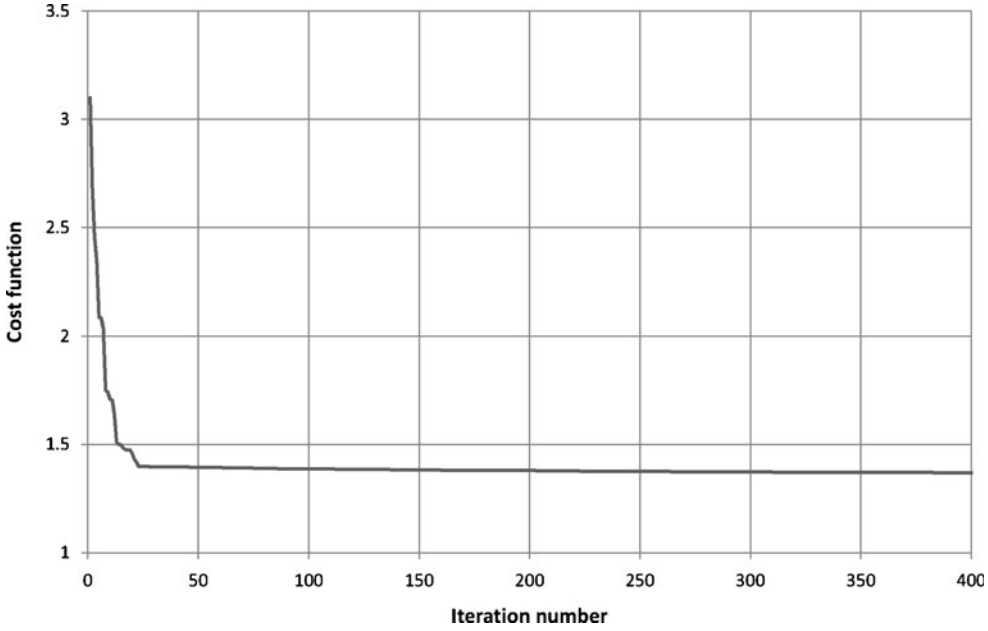

Fig. 5 Reduction of the cost function during iterations

To find an estimate for the parameter C, the cuboid was fixed at a given position and the distance, separating the two holes, was measured 16 times. Every time the CMM was returned to a home position before the arm was extended to take the measurement. The value of C was then set equal to the standard deviation of the repeatability error. On the other hand, after a number of trial runs, R has been set equal to 0.000002.

If Θ_q is an entry of Ω, the constraints imposed on its value (i.e. $\Theta_q|_{\max}$ and $\Theta_q|_{\min}$) are incorporated in the procedure, as suggested by Kothandaraman and Rotea [9], as follows:

$$\Theta_q^{k+1} = \begin{cases} \Theta_q|_{\max} \text{ if } \Theta_q^{k+1} > \Theta_q|_{\max} \\ \Theta_q|_{\min} \text{ if } \Theta_q^{k+1} < \Theta_q|_{\min} \end{cases} \quad (16)$$

In the present analysis, only the distance D was constrained to remain within the range of 39.80 to 40.20 mm. The manufacturer had previously indicated that the actual value of this distance was 40.05 mm, and this was the value confirmed by the optimisation procedure. The fact that the solution obtained is fully interior suggests that the optimality condition has not been violated as a result of applying the approach shown in Eq. 16.

5 Experimental results

The initial values assigned to the model parameters have been acquired from the data provided by the manufacturer. These values are given in Table 1.

The calibration region was constrained to a horizontal base plate in the work volume of the CMM. The cuboid was fixed, at random planar orientations, to a total of 45 positions

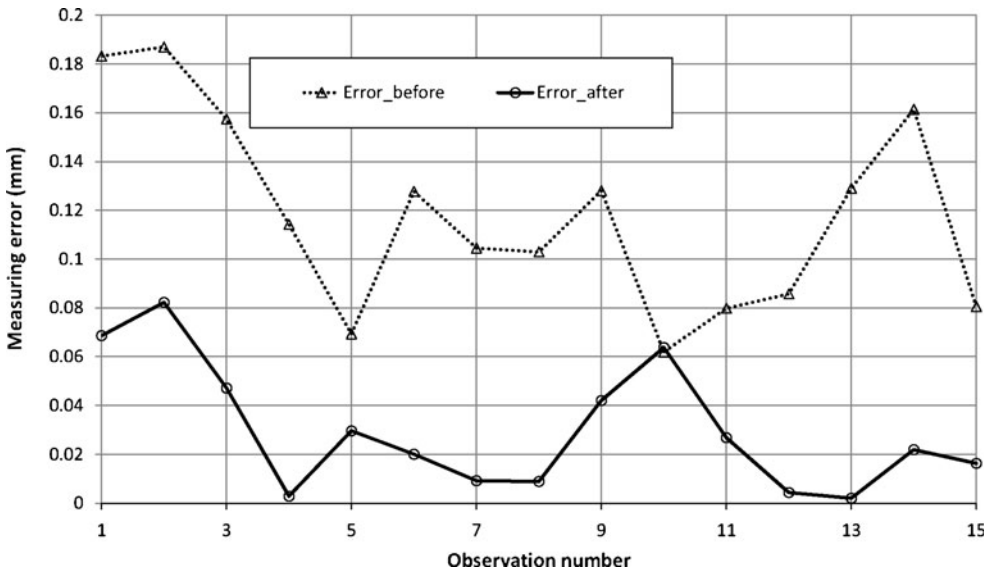

Fig. 6 Measurement error before and after calibration

(i.e. M=45 as per Eq. 13) whereby, at each location, the stylus was inserted into the two holes to calculate the error function, $E_j(\Theta)$. The reported sensor readings, θ_i, have been noted and used in the mathematical procedure. Even though 700 iterations were allowed for the stochastic optimisation procedure, convergence was realised long before this number was reached. The resulting values for the systems parameters are given in Table 2, and the values calculated for the cost function during the course of the procedure are given in Fig. 5.

The calibrated system parameters obtained in this analysis have been substituted in the CMM mathematical model, and the machine was then used to measure the distance between the two cuboid holes at 15 new fixture locations situated in the measuring space. The error values produced by these 15 measurements are depicted in Fig. 6 together with the corresponding error values obtained by the uncalibrated kinematic model. The figure asserts the considerable accuracy improvement produced by the adopted procedure. The mean measurement error has been reduced from 0.1182 to 0.0297 mm, and the standard deviation of error has been reduced from 0.04 to 0.026 mm.

6 Conclusions

In this paper, a simple method for the calibration of a serial manipulator-like CMM has been proposed and demonstrated experimentally. The method does not require the use of expensive measuring equipment to collect position data. The mathematical model employed for the analysis utilises the well-known DH parameters combined with a stochastic optimisation approach. In the model, sensor offsets have also been accounted for by a linear expression which relates the actual joint angle to its reported value. The calibration procedure presented in this paper considerably improves the accuracy, of an already accurate device, which proves the validity of the proposed approach and its suitability for the discussed application.

Acknowledgements The authors would like to acknowledge the information received from the Immersion Corporation staff, Mr Bill Hoverter and Mr. Nemer Velasquez.

References

1. Bai Y, Wang D (2006) Fuzzy logic for robots calibration—using fuzzy interpolation technique in modeless robot calibration. In: Bai Y, Zhuang H, Wang D (eds) Advanced fuzzy logic technologies in industrial applications. Springer, London
2. Denavit J, Hartenberg RS (1955) A kinematic notation for low pair mechanisms based on matrices. ASME J Appl Mech 22:215–221
3. Driels MR, Pathre US (1991) Vision based automatic theodolite for robot calibration. IEEE Trans Robot Autom 7(3)
4. Foulloy LP, Kelly RB (1984) Improving the precision of a robot. In: Proc. IEEE Conf. Robotics., pp 62–67
5. Immersion Corporation (2000) MicroScribe 3D Desktop Digitizing Systems: user's guide & set-up instructions. Immersion Corporation, San Jose
6. Immersion Corporation (2004) MicroScribe API 2.2 user reference. Immersion Corporation, San Jose
7. Judd RP, Knasinsky AB (1987) A technique to calibrate industrial robots with experimental verification. In: Proc. IEEE Conf. Robotics., pp 351–357
8. Khalil W, Besnard S (2002) Geometric calibration of robots with flexible joints and links. J Intell Robot Syst 34:357–359
9. Kothandaraman G, Rotea MA (2005) Simultaneous-perturbation stochastic-approximation algorithm for parachute parameter estimation. J Aircr 42(5):1229–1235
10. Lim C, Burdekin MM (2002) Rapid volumetric calibration of coordinate measuring machines using a hole bar artefact. Inst Mech Eng B J Eng Manuf 216:1083–1093
11. Mooring BW, Roth ZS, Driels MR (1991) Fundamentals of manipulator calibration. Wiley, New York
12. Reisner LA, King BW, Klein MD, Auner GW, Pandya AK (2007) A prototype biosensor-integrated image-guided surgery system. Int J Med Robot Comput Assist Surg 3(1):82–88
13. Schena BM, Rosenberg LB (1997) Mechanical digitising arm used to input three dimensional data into a computer. US patent no. Des.337,932
14. Spall JC (1992) Multivariate stochastic approximation using a simultaneous perturbation gradient approximation. IEEE Trans Autom Control 37(3):332–340
15. Spall JC (1998) Implementation of the simultaneous perturbation algorithm for stochastic optimization. IEEE Trans Aerosp Electron Syst 34(3):817–823
16. Sultan IA, Wager JG (1999) User-controlled kinematic modelling. Int J Adv Robot 12(6):663–677
17. Sultan IA, Wager JG (2001) A technique for the independent-axis calibration of robot manipulators with experimental verification. Int J Comput Integr Manuf 14(4)
18. Veitschegger WK, Wu CH (1987) A method for calibrating and compensating robot kinematic errors. In: Proc. IEEE Conf. Robotics Automation., pp 39–44